JOURNAL OF GEOPHYSICAL RESEARCH, VOL. 106, NO. A11, PAGES 24,843–24,855, NOVEMBER 1, 2001

The elementary current method for calculating ionospheric current systems from multisatellite and ground magnetometer data

O. Amm

Geophysical Research Division, Finnish Meteorological Institute, Helsinki, Finland

Abstract. The recently launched Cluster II mission provides for the first time the possibility to instantaneously obtain spatially distributed measurements of field-aligned currents from a fleet of satellites. We present the "elementary current method" that combines such measurements mapped to the ionosphere with two-dimensional ground magnetic data, to calculate actual (not equivalent) ionospheric currents, without the need of further assumptions. If additional two- dimensional measurements of the ionospheric electric field from coherent scatter radars are available, the ionospheric Hall and Pedersen conductances can also be inferred. The applicability of the method is demonstrated for a passage of the Cluster II spacecraft over the Multi-Instrument Array for Ionosphere-Magnetosphere Coupling Studies (MIRACLE) network of ground-based instruments in northern Fennoscandia on February 1, 2001, using preliminary but realistic orbit parameters. The geophysical situation of ionospheric electrodynamic parameters that we model during this passage refers to a real event of a plasma vortex propagating eastward over the MIRACLE field of view, as studied by *Kosch et al.* [2000]. The application of the elementary current method to the simulated ground magnetometer and satellite measurements calculated from this model shows that the modeled ionospheric currents, as well as the Hall and Pedersen conductances, can be reconstructed by the method to good accuracy.

1. Introduction

Ground-based support is crucial even for a multispacecraft mission in the magnetosphere to obtain information on the medium- and global-scale plasma environment the satellites are located in. Such support can be provided by networks of magnetometers, radars, all-sky cameras, and other ground-based instruments. During and after the International Magnetospheric Study (IMS, 1976-1979), several methods were developed to obtain spatial, instantaneous distributions of the macroscopic electrodynamic parameters of the ionosphere from ground-based measurements [e.g., *Akasofu et al.*, 1980; *Kamide et al.*, 1982] (see the review of *Untiedt and Baumjohann* [1993] for methods used for data from Scandinavia). Mostly, the ground magnetic field disturbances measured by magnetometers are the main input quantities to these methods, supported by ionospheric electric field data measured by radars and optical data, when available.

Since no spatial, instantaneous measurements from satellites, for example, of the field-aligned current (FAC) distribution, have been available, satellite data were mainly used for comparison to the ionospheric results [e.g., *Sulzbacher et al.*, 1982], or as statistically derived distributions using many satellite passes [e.g., *Rich and Kamide*, 1983]. Under favorable geometrical circumstances the four Cluster II satellites now offer the possibility to infer such FAC distributions mapped to the ionosphere, thus giving the opportunity to enhance the analysis methods with this input quantity.

In this paper we present the "elementary current method" (ECM) that utilizes this input together with ground magnetic field data to infer actual (not equivalent) ionospheric currents without additional assumptions, even in the case that the ionospheric electric field is unknown. This considerably improves the applicability of the method, since although coherent scatter radars now cover a large area in the Northern Hemisphere, there are circumstances under which they do not receive sufficient backscatter. In addition, if spatial measurements of the ionospheric electric field are available on the same area, the ionospheric conductances can also be calculated. In section 2, the new method is put into the context of existing analysis methods that use ground-based and/or satellite-based data to infer distributions of ionospheric electrodynamic parameters. Section 3 presents the theoretical background of the ECM. In section 4 we apply our new method to an ionospheric electrodynamic situation of a plasma vortex, modeled referring to a real event studied by *Kosch et al.* [2000], using realistic Cluster II orbit parameters and magnetometer locations, in order to test how accurately the method is able to reconstruct the modeled input.

Paper number 2001JA900021.
0148-0227/01/2001JA900021$09.00

2. Overview of Methods to Infer Spatial Distributions of Ionospheric Electrodynamic Parameters

Table 1 shows the basic properties of selected methods to infer the macroscopic ionospheric electrodynamic parameters from ground-based and/or satellite data. The full parameter set that is intended to be measured or calculated consists of the ionospheric electric field $\vec{E}$ or electric potential Φ_E, the Hall and Pedersen conductances Σ_H and Σ_P, the horizontal ionospheric sheet current density $\vec{J}$, and the FACs $j_\parallel$.

First we note that from measurements of the ground magnetic field disturbance $\vec{B}_G$ alone, we can derive only equivalent ionospheric currents $\vec{J}_{eq,ion}$ from an upward field continuation

Table 1. Overview of Selected Methods to Derive Macroscopic Ionospheric Electrodynamic Parameters From Ground-based and Satellite Data[a]

Input	Assumptions	Output	Name of Method	Remarks
$\vec{B}_G$	-	$\vec{J}_{eq,Ion}$	field continuation	forward method no true currents, no FACs
$\vec{B}_G$	Σ_H, Σ_P	$\vec{E}$ (Φ_E), $\vec{J}$, $j_\parallel$	KRM	forward method boundary conditions critical if non-global
$\vec{B}_G$, {$\vec{E}$ (Φ_E), satellite data}	Σ_H, Σ_P	{$\vec{E}$ (Φ_E)}, $\vec{J}$, $j_\parallel$	AMIE, "three-dimensional modeling"	assimilation method (least square or "trial and error"); data need not to cover whole analysis area
$\vec{B}_G$, $\vec{E}$	$\alpha = \Sigma_H/\Sigma_P$	Σ_H, Σ_P, $\vec{J}$, $j_\parallel$	method of characteristics	forward method α assessible from all-sky camera data or from $\vec{B}_G$
$j_\parallel$	Σ_H, Σ_P	$\vec{E}$ (Φ_E), $\vec{J}$	-	forward method boundary conditions critical if non-global
$j_\parallel$, $\vec{B}_G$, {$\vec{E}$}	-	$\vec{J}$, {Σ_H, Σ_P}	elementary current method	forward method

[a]FACs, Field-aligned currents; KRM, Kamide-Richmond-Matsushita algorithm; AMIE, assimilative mapping of ionospheric electrodynamics.

procedure, and not the true currents $\vec{J}$. Since $\vec{J}_{eq,ion}$ is divergence-free, no conclusions regarding the FACs can be drawn from it, unless uniform ionospheric conductances are assumed [cf. *Untiedt and Baumjohann*, 1993].

When a model for the ionospheric conductances is added, Φ_E can be calculated by solving a second-order partial differential equation. This approach is known as the Kamide-Richmond-Matsushita (KRM) method [*Kamide et al.*, 1981]. While the KRM method has successfully been applied to global scale studies, for regional analyses the unknown boundary conditions cause substantial uncertainty in the results [*Murison et al.*, 1985].

The assimilated mapping of ionospheric electrodynamics (AMIE) procedure [*Richmond and Kamide*, 1988] is one of the most commonly used methods for deriving ionospheric electrodynamics. In contrast to KRM and all other methods mentioned in this overview, AMIE is an assimilation method, that is, the unknown electrodynamic parameters are selected in a way such that they provide the best consistency with all available measurements, using a least squares approach. This gives AMIE the flexibility to utilize many different data sets, and every input data set does not have to cover the full analysis region, which is not the case for forward methods that are based on the solution of algebraic or differential equations. On the other hand, the AMIE procedure requires the distributions of both ionospheric conductances as input. Although the method can make use of directly measured conductance data, such data are typically not available, especially not on the global scale to which AMIE is applied. Therefore the conductances need usually to be taken from statistically based models and other statistical "a priori" information, which reduces the method's ability to adequately represent single events. Moreover, it is not easy to estimate the uncertainty of the results in regions where the density of actual data is sparse. Until now, AMIE is only available for global-scale analyses.

Other modeling approaches for the three-dimensional ionospheric current system on global and regional-scales, although usually technically not as advanced, are qualitatively similar to the AMIE method. During the IMS period the "trial and error method" was frequently used in regional scale studies [e.g., *Baumjohann et al.*, 1981; *Opgenoorth et al.*, 1983]: Models for the desired electrodynamic quantities were improved on a heuristic basis until sufficient agreement between measurements and their values predicted from the model was achieved.

The method of characteristics [*Inhester et al.*, 1992; *Amm*, 1995, 1998] uses measurements of $\vec{B}_G$ and $\vec{E}$ to derive the full set of electrodynamic parameters. Unlike the previous techniques, it needs an estimate of the distribution of the Hall to Pedersen conductance ratio $\alpha = \Sigma_H/\Sigma_P$ only. *Lester et al.* [1996] have shown that this ratio, in contrast to Σ_H and Σ_P, shows a relatively stable relation to the ground magnetic disturbance level and is therefore more easily assessible. In addition, *Amm* [1995] found that the results of the method are robust with respect to the estimate of α as well as to the boundary conditions.

Two, in principle different, possibilities exist to obtain spatial distributions of FACs ($j_\parallel$) from satellite measurements: First a large number of passes from one or from several but not nearby located satellites can be grouped together to a statistical database with respect to magnetic local time (MLT) and latitude and possibly binned according to other parameters like *Kp* or the interplanetary magnetic field (IMF). This approach has been used since the 1960s, the most well-known result being the classical paper of *Iijima and Potemra* [1978]. However, because of its statistical nature it is not suitable for studies of characteristics during individual events.

Second a fleet of nearby located satellites can provide multipoint measurements of a limited region, such as is now the case with Cluster II. Because four data points at the satellites' ionospheric footpoints alone are usually not sufficient to infer two-dimensional FAC distributions in an extended ionospheric region, two cases are of special interest: Either a feature to be analyzed moves across the satellite footpoints' area, which can be assumed to be stationary, or the satellites' footpoints move over a stationary feature. To construct spatial FAC distributions, in the first case the footpoints must not be lined up in the direction of the features' motion; in the second case they must not be lined up in the direction of the satellite motions. In both cases, data from different time steps is translated to a reference time step, with respect to the motion of the feature or the footpoints. Thus the condition of instantaneous data analysis is slightly relaxed to a "quasi-instantaneous" condition. However, the time interval for which stationarity of the feature has to be assumed can be adjusted by a proper selection of the size of the analysis region.

Some uncertainty in the FAC estimation may be introduced by the FAC calculation from each satellite when interpreting the magnetic field data in terms of infinite current sheets, by the field line mapping procedure and by possible field-aligned potential

drops. However, these factors have to be checked in each individual case, and they are not further discussed in this paper. Hence, in the following we assume that the representative $j_\parallel$ values at the satellites' footpoints have been obtained from the satellite data.

If only $j_\parallel$ is known, the full electrodynamic parameter set can be obtained by assuming a model for Σ_H and Σ_P and by integrating a second-order partial differential equation for Φ_E (the same technique as used, e.g., by *Rich and Kamide* [1983]). Like with the KRM method, this approach works well for global analysis regions, but unknown boundary conditions are a major problem when trying to apply it to regional studies. Since, as pointed out above, quasi-instantaneous $j_\parallel$ distributions are not available on a global scale, this approach is of minor significance for the Cluster II analysis.

If additional knowledge of $\vec{B}_G$ is available, the "elementary current method" (ECM) that is presented in this paper can be utilized to calculate $\vec{J}$ without any integration needed, by expanding $\vec{J}$ into curl-free and divergence-free spherical elementary current systems (SECS) [see *Amm*, 1997]. In case that also $\vec{E}$ is measured, the Hall and Pedersen conductances can immediately be calculated from this result. None of the input distributions has to be assumed.

3. Elementary Current Method: Theory

As known from Helmholtz's theorem, any vector field can be split into a curl-free (subscript "cf") and a divergence-free (subscript "df") part, so that the ionospheric currents $\vec{J}$ can be written in the form

$$\vec{J} = \vec{J}_{cf} + \vec{J}_{df} . \tag{1}$$

From measurements of $\vec{B}_G$ and $j_\parallel$ and after applying an upward field continuation procedure to calculate $\vec{J}_{eq,ion}$ from $\vec{B}_G$ [e.g., *Amm and Viljanen*, 1999], by virtue of

$$\nabla_h \cdot \vec{J} = \nabla_h \cdot \vec{J}_{cf} = j_\parallel \tag{2}$$

and

$$\nabla_h \times \vec{J} = \nabla_h \times \vec{J}_{df} = \nabla_h \times \vec{J}_{eq,ion} , \tag{3}$$

we know the curl and divergence of $\vec{J}$. This knowledge could be used to integrate $\vec{J}$ using standard techniques to solve sets of partial differential equations, like the finite difference method, and imposing (actually unknown) boundary conditions. However, it is much easier to solve (2) and (3) without the need of any integration by composing $\vec{J}$ of curl-free and divergence-free SECS [see *Amm*, 1997]. These elementary systems are sketched in Figure 1. Besides the fact that one system is curl-free, and the is other divergence-free, they have a unit curl or divergence at their origin ("pole"), respectively, and can therefore be used as elementary solutions to (2) and (3). As shown by *Amm* [1997], any current system $\vec{J}$ can uniquely be decomposed as integrals over SECS as

$$\vec{J}(\vec{r}) = \iint_{\text{Ionosph}} \left(\frac{\left[\nabla_h \times \vec{J}(\vec{r}')\right]_r}{4\pi R_I} \cot(\tilde{\vartheta}/2)\, \underline{e}_{\tilde{\varphi}} + \frac{\nabla_h \cdot \vec{J}(\vec{r}')}{4\pi R_I} \cot(\tilde{\vartheta}/2)\, \underline{e}_{\tilde{\vartheta}} \right) d^2r' . \tag{4}$$

In (4), $\tilde{\vartheta}$ and $\tilde{\varphi}$ are spherical coordinates with respect to the pole of each elementary system, $\underline{e}_{\tilde{\vartheta}}$ and $\underline{e}_{\tilde{\varphi}}$ are the unit vectors in these directions, and R_I is the radius of the ionosphere ($R_I = R_E + 100$ km, with R_E being the Earth's radius). During the integration the vectors inside the brackets which are expressed in the $(\vec{r}, \tilde{\vartheta}, \tilde{\varphi})$ coordinate system of each individual elementary system, have to be transformed into the coordinate system of $\vec{r}$ and $\vec{r}'$ (usually geographic or geomagnetic). Hence, with (4), $\vec{J}$ can directly be composed from its curls and divergences. However, parts of $\vec{J}$ that contain neither divergences nor curls inside the analysis area will not be represented. Therefore it is important that the analysis area includes the essential FAC systems that cause the horizontal currents.

When dealing with quantities given on a regular grid rather than with continuous functions as in (4), the expansion of $\vec{J}$ is written as

$$\vec{J}(\vec{r}) = \sum_i \left(\frac{I_{0,df,i}}{4\pi R_I} \cot(\tilde{\vartheta}/2)\, \underline{e}_{\tilde{\varphi}} + \frac{I_{0,cf,i}}{4\pi R_I} \cot(\tilde{\vartheta}/2)\, \underline{e}_{\tilde{\vartheta}} \right) , \tag{5}$$

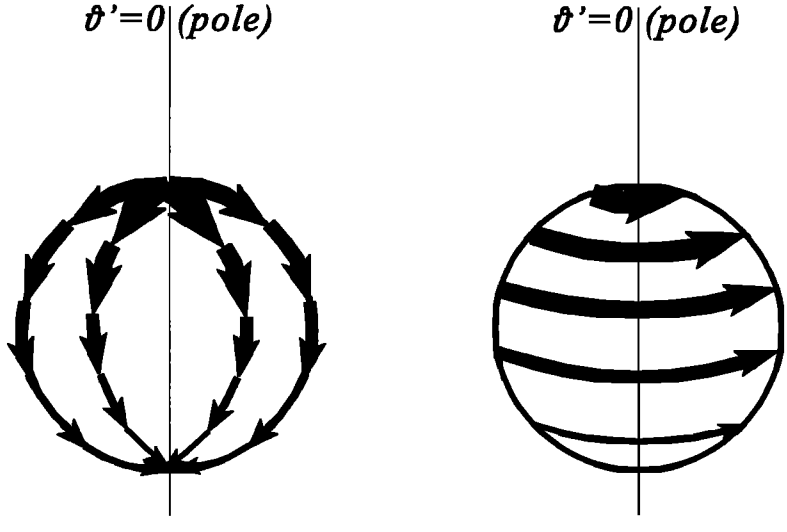

Figure 1. Sketch of the spherical curl-free and divergence-free elementary current systems used for the elementary current method.

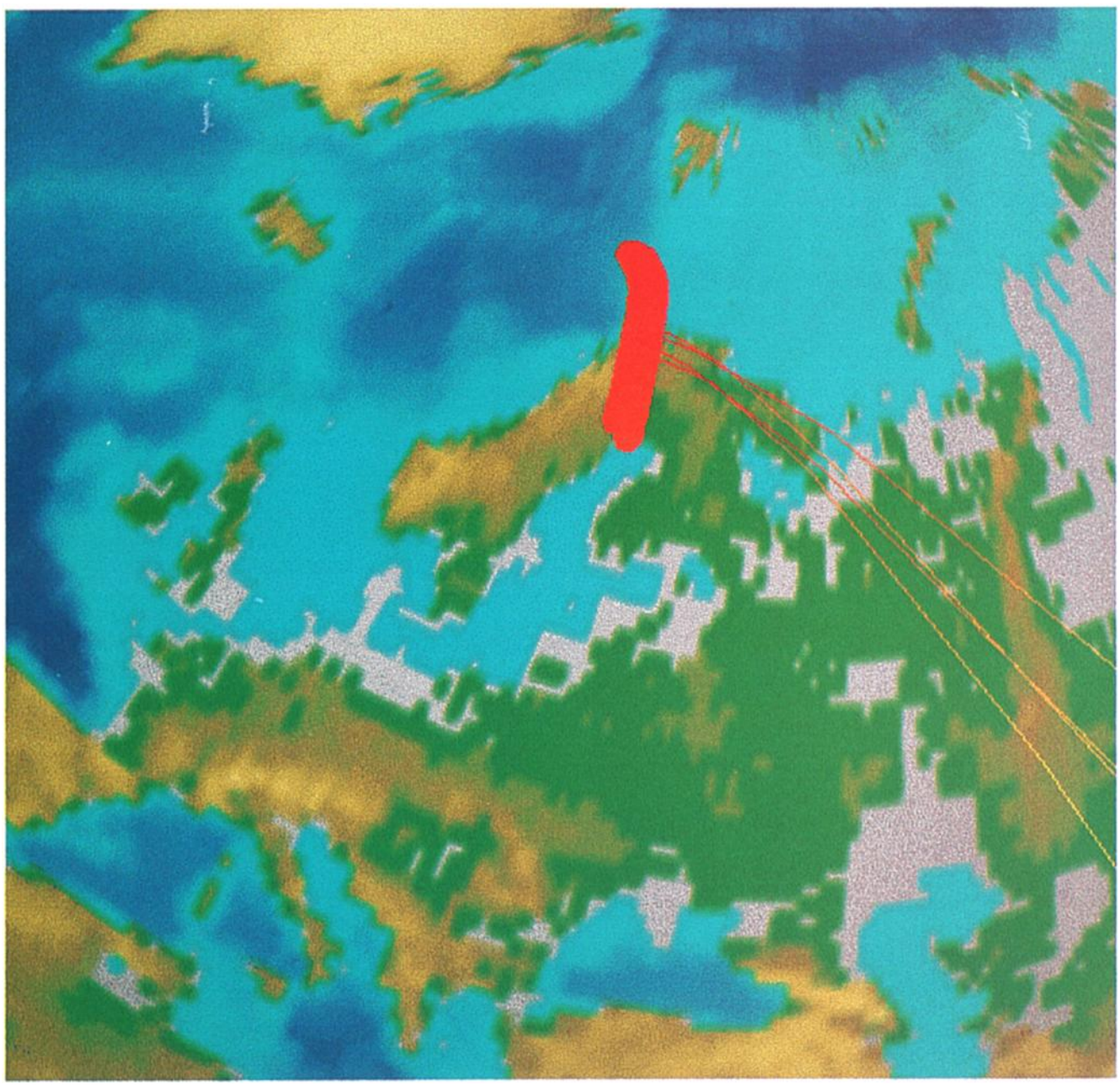

Plate 1. Cluster II magnetic footpoint geometry during a passage over northern Scandinavia on February 1, 2001, between 2030 and 2100 UT (thick red lines). Additionally, the four conjugate field lines of the satellites for the reference time step of our analysis, 2045:30 UT, are shown.

where $i = 1,...,N$ is a counting index of the grid points where poles of SECS are placed. The scaling factors $I_{0,\left[\begin{smallmatrix}cf\\df\end{smallmatrix}\right],i}$ at the position of grid point i are calculated as

$$I_{0,cf,i} = \iint_{F_i} \nabla_h \cdot \vec{J}(\vec{r}') \, d^2r' \,, \tag{6}$$

$$I_{0,df,i} = \iint_{F_i} \left[\nabla \times \vec{J}(\vec{r}')\right]_r \, d^2r' \,, \tag{7}$$

with F_i being the grid point area around grid point i. Typically, the integrand in (6) and (7) is regarded as a constant within each grid point area.

Once $\vec{J}$ is known from (4) or (5), with measurement of $\vec{E}$ the conductances are straightforwardly derived from Ohm's law to

$$\Sigma_H = \frac{(\vec{J} \times \vec{E})_r}{|\vec{E}|^2} \quad ; \quad \Sigma_P = \frac{\vec{J} \cdot \vec{E}}{|\vec{E}|^2} \,. \tag{8}$$

These equations have been derived under the assumption that the magnetic field lines are directed perpendicular to the ionospheric plane. If they are not, the conductance tensor gets off-diagonal elements, and polarization effects have to be included (for an exact treatment, see, e.g., *Amm* [1996]). Still, (8) is a very good approximation for small inclination angles, as in the polar ionosphere to which Cluster II is conjugate. The sign of the equation for Σ_H is the one valid in the Northern Hemisphere.

Note that in the case that no measurements of $\vec{E}$ are available, $\vec{J}$ can still be derived with (4) or (5) as described above. Then, either $\vec{E}$ can be inferred by assuming distributions of Σ_H and Σ_P, or vice versa. In the first case the multitude of possible Σ_H and Σ_P models can be restricted by the assertion that $\vec{E}$ is curl-free. In the second case the condition that Σ_H and Σ_P are nonnegative can be used to restrict the choice of a model for $\vec{E}$.

4. Application Example of the Elementary Current Method With a Model of a Real Event and Realistic Cluster II Orbit Geometry

We test the elementary current method (ECM) using a model of a real event of a plasma vortex that passed over northern Scandinavia on January 15, 1980, at 2135 UT. This event has recently been described and analyzed by *Kosch et al.* [2000], who derived two-dimensional distributions of conductances, horizontal ionospheric currents, and FACs for one time step of the vortex passage, using the method of characteristics (see section 2). Using a conjunction of the Cluster II satellite fleet with the MIRACLE network of ground-based instruments on February 1, 2001, around 2045 UT, we reconstruct the measurements that the satellites and the ground magnetometers of the International Monitor for Auroral Geomagnetic Effects (IMAGE) network would observe during the plasma vortex event. Using these data as input, we apply the ECM and inspect how well its results can reproduce the modeled input distributions.

While we try to make our test of the ECM as realistic as possible by using both a realistic ionospheric electrodynamic situation as well as a realistic Cluster II orbit situation, it should be emphasized that the main purpose of this paper is to test the method as such, and neither the special geographic locations nor the special type of event chosen as a test example is of particular importance and will therefore not be discussed in great detail.

Plate 1 shows the footpoints of the Cluster II spacecraft over Fennoscandia on February 1, 2001, between 2030 and 2100 UT, as calculated with the Orbital Visualisation Tool (OVT), using preliminary Cluster II orbit parameters and the Tsyganenko 87 model with $Kp=1_+$ (the value during the event of *Kosch et al.* [2000]) for the mapping procedure. The satellites' footpoints move southward over northern Scandinavia with a speed of ~ 0.27° latitude per minute, being almost in a meridonal line configuration, with a latitudinal spacing of ~ 0.1°-0.6°. Additionally, the satellites' four conjugate field lines are shown for 2045:30 UT, which is the central time step in our event analysis below. Figure 2 displays the MIRACLE network of ground-based instruments which has its densest two-dimensional coverage in the northernmost parts of Finland, Sweden, and Norway. The network consists of the IMAGE magnetometers, the Scandinavian Twin Auroral Radar Experiment (STARE) coherent scatter radar, and several all-sky cameras [*Syrjäsuo et al.*, 1998]. The field of view in which STARE can measure the ionospheric electric field is indicated with a frame.

In Figure 3, the model of a plasma vortex used for our test is shown. The model parameters are fitted with simple analytical functions to the results of the event study by *Kosch et al.* [2000] and comprise all main features of the vortex that resulted from that analysis. Note that in their event, an arc was present equatorward of the plasma vortex, as well as some auroral activity in the northwestern edge of the analysis region. For simplicity, these features are not included in our model. The modeled vortex, in agreement with the real one, moves eastward with a velocity of 4 km s^{-1}, as inferred both from all-sky camera and from magnetometer observations. The geographic positions shown in Figure 3 correspond to the vortex position at the central time step at 2045:30 UT. We assume that the vortex is stationary during its motion over the central MIRACLE field of view, i.e., for ~ 2 min. Since the satellites' footpoints move very little during this interval, we have the situation mentioned in section 2 that a feature moves over nearly fixed satellites' footpoints, which are in this case almost perpendicularly aligned to the feature's direction of motion. This situation allows us to combine data during different timesteps and translate them to the reference time step t_{ref} using the velocity of the vortex $\vec{v}_{vortex}$. That is, if the satellite measures a field-aligned current density $j_\parallel$ at a position $\vec{r}$ and a time $t \neq t_{ref}$, we can write $j_\parallel(\vec{r},t) = j_\parallel[\vec{r} - \vec{v}_{vortex}(t - t_{ref}), t_{ref}]$.

The electric field $\vec{E}$ of the plasma vortex is directed radially away from its center, located at 69° latitude and 21° longitude at 2045:30 UT (Figure 3a). This is equivalent to an anticlockwise vortex of plasma flow. Corresponding to the finding of *Kosch et al.* [2000], the vortex center is associated with a minimum both in Σ_H and in Σ_P (Figures 3b and 3c). At the center, Σ_H amounts to 4 S, from where it increases isotropically to ~ 8 S at the boundaries of the modeling area. The ratio Σ_H/Σ_P is fixed to 1.5 throughout this area. The ionospheric current system $\vec{J}$ is a clockwise-directed spiral emerging out of the vortex center, with sheet current density magnitudes increasing from 45 mA m^{-1} at the center to ~ 110 mA m^{-1} at the boundaries of the modeling region (Figure 3d). Consequently, to feed these horizontal currents a patch of downward flowing FACs is located inside the plasma vortex, with a maximum magnitude of 1.5 A km^{-2}, decreasing from the center

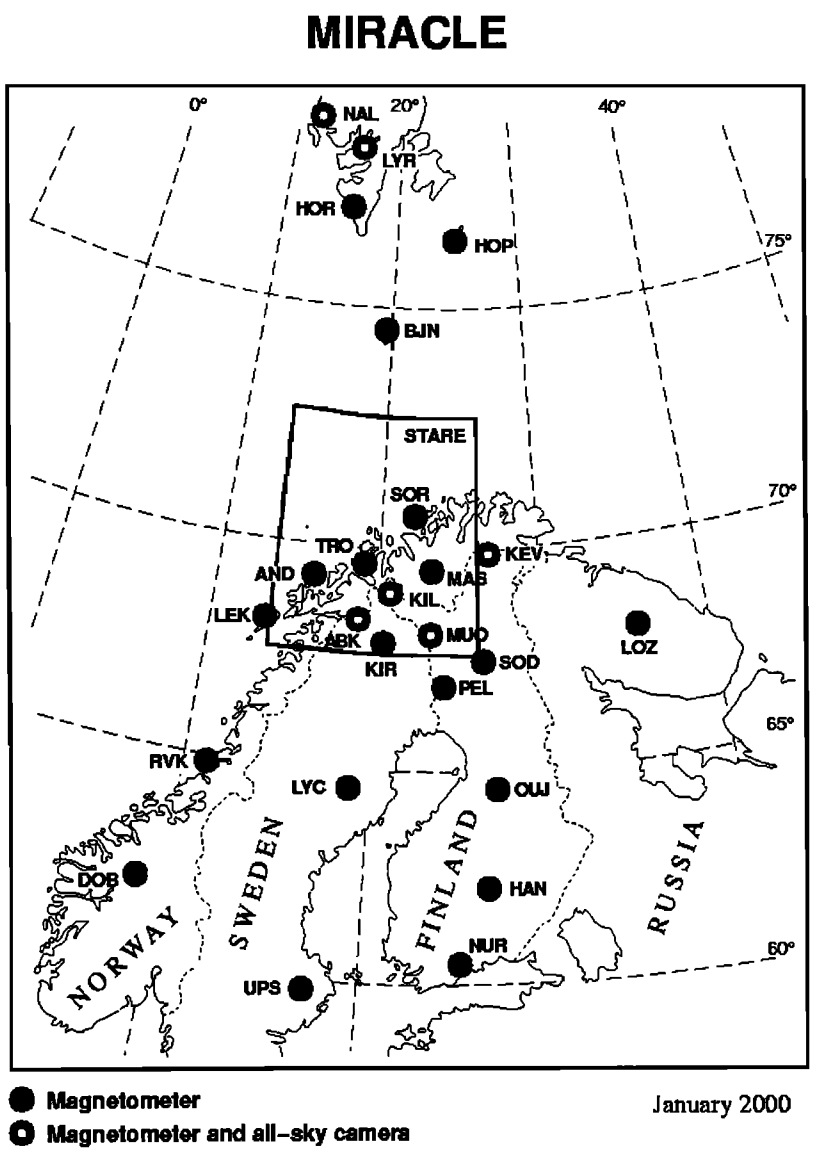

Figure 2. The MIRACLE network of ground-based instruments in Fennoscandia. Circles: Magnetometer and all-sky camera stations (full station names and coordinates can be found at *http://www.geo.fmi.fi/image/coordinates.html*); Rectangular frame: Field of view of the STARE coherent scatter radar.

outward (Figure 3e). For later comparison with the results of the ECM, Figures 3f and 3g show the curl-free and divergence-free current parts, $\vec{J}_{cf}$ and $\vec{J}_{df}$, as computed directly from the model. In our case, $\vec{J}_{cf}$ has a radial structure, and $\vec{J}_{df}$ has a circular structure with respect to the vortex center. $\vec{J}_{df}$ is equal to the equivalent currents immediately below the ionospheric plane, $\vec{J}_{eq,ion}$. Note that the equivalent currents thus differ remarkably from the true current system $\vec{J}$ shown in Figure 3d.

The simulated FAC and ground magnetometer observations following from this model and the Cluster II orbit geometry are shown in Figure 4. In Figure 4a, the FACs seen by the four Cluster II spacecraft during the passage of the vortex have been mapped to the reference timestep 2045:30 UT, taking into account both the satellite footpoints and the vortex motion, with a temporal resolution of 1 s. Since we neglect possible errors inherent to the satellite measurements and the mapping procedure as discussed in section 2, the FAC values shown in Figure 4a are directly interpolated from the "true," modeled FAC distribution (Figure 3e) to the respective footpoint locations. The resulting four traversals through the vortex FAC structure well expose the downward FAC accumulation near its center and the decreasing current intensities away from the center. Naturally, longtudinal gradients are better resolved in this geometry than are the latitudinal ones. The simulated IMAGE ground magnetometer measurements at the reference time step are displayed in Figure 4b. The vectors represent the horizontal magnetic disturbance rotated clockwise by 90°, that approximately point in the direction of the equivalent currents on the ground. They exhibit a similar circular structure as $\vec{J}_{eq,ion}$ (compare with Figure 3g). The numbers at each vector origin are the vertical magnetic disturbances, positive downward. At the station Kilpisjärvi (KIL) (see Figure 2) close to the center of the vortex, a maximum vertical disturbance of ~ 74 nT is observed.

The simulated data shown in Figure 4 are then used as input to the ECM. First the FAC measurements (Figure 4a) are interpolated

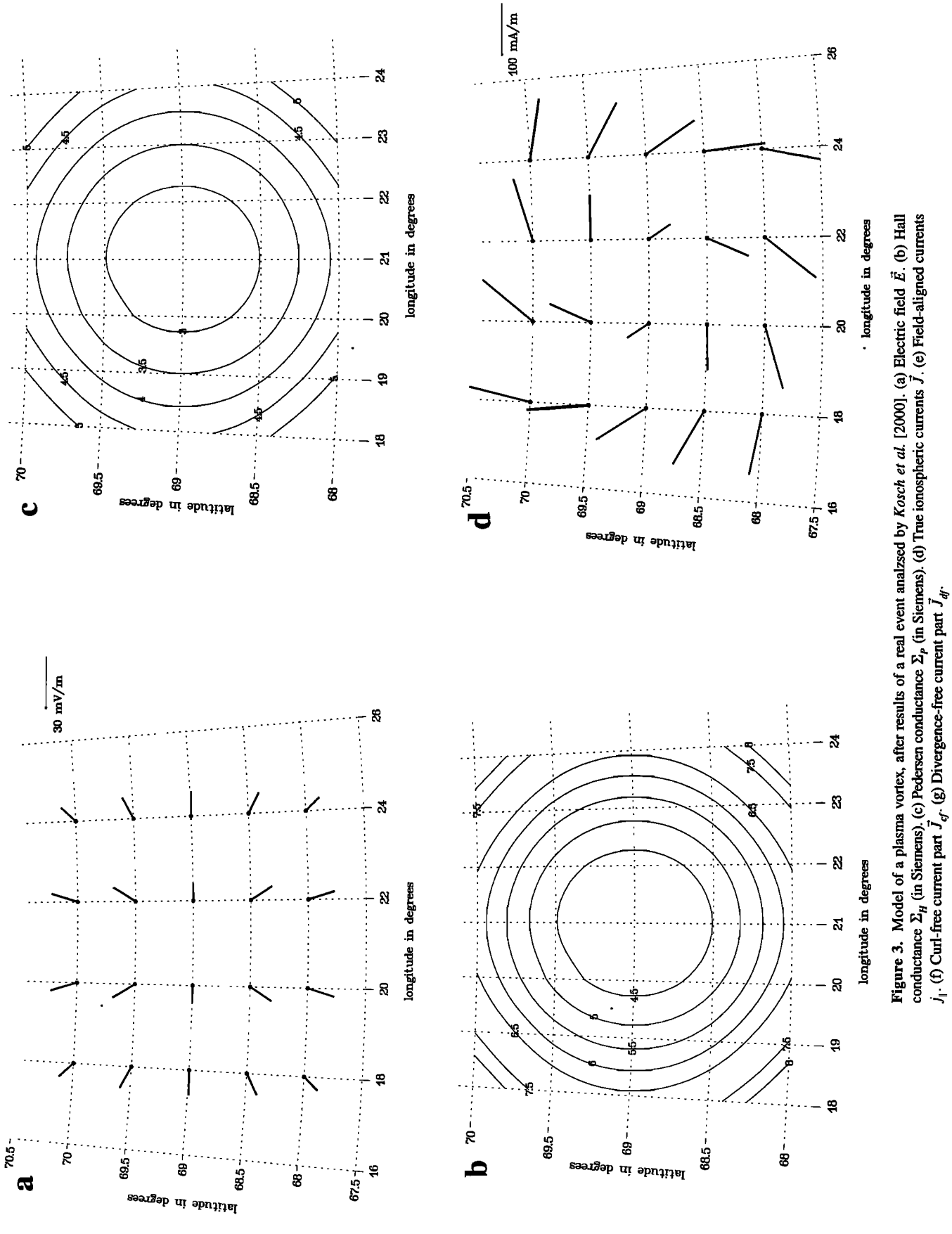

Figure 3. Model of a plasma vortex, after results of a real event analzsed by *Kosch et al.* [2000]. (a) Electric field $\vec{E}$. (b) Hall conductance Σ_H (in Siemens). (c) Pedersen conductance Σ_P (in Siemens). (d) True ionospheric currents $\vec{J}$. (e) Field-aligned currents $j_\parallel$. (f) Curl-free current part $\vec{J}_{cf}$. (g) Divergence-free current part $\vec{J}_{df}$.

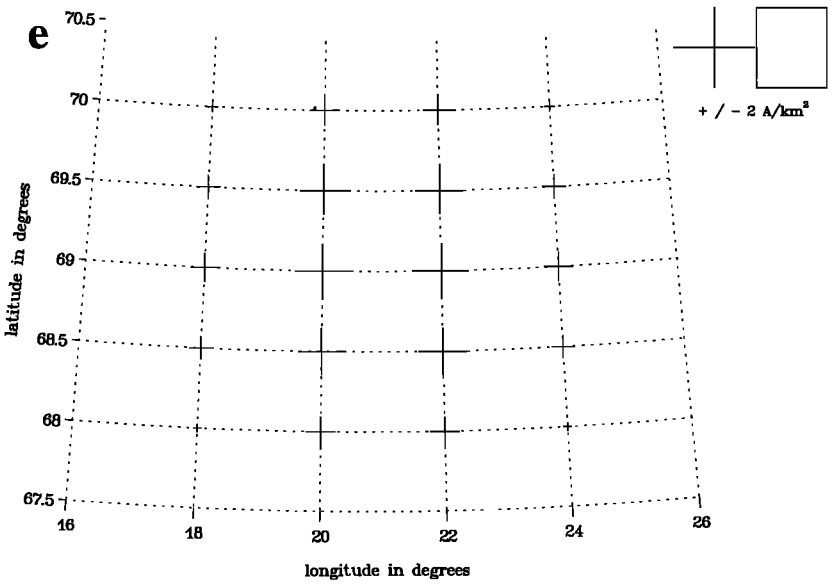

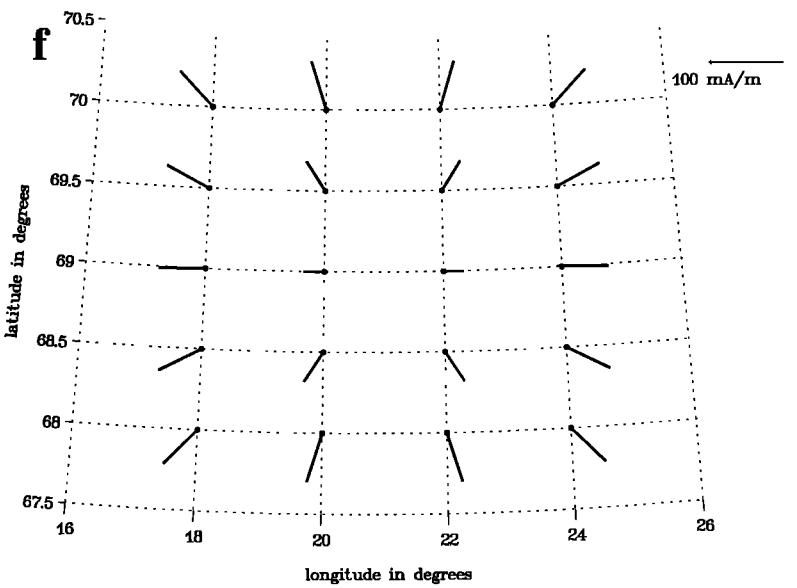

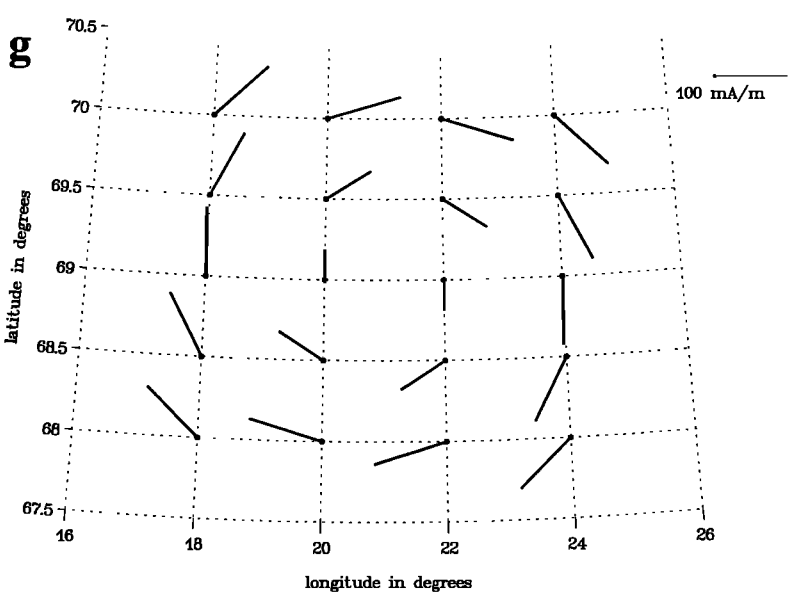

Figure 3. (continued)

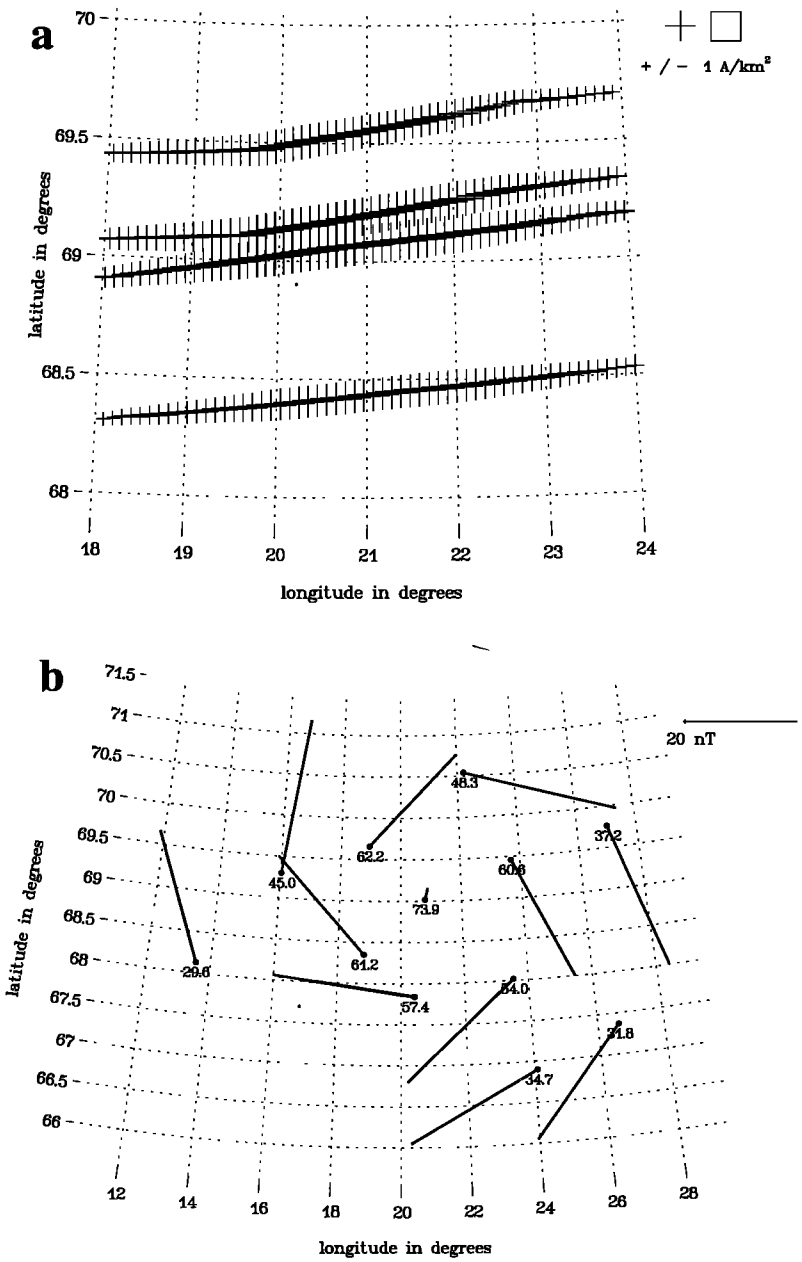

Figure 4. Simulated measurements following from the model, as used as input data to the elementary current method. (a) Field-aligned currents from the four Cluster II satellites, mapped to the reference timestep 2045:30 UT, with respect to the velocity of the vortex and the satellites' magnetic footpoints. (b) Ground magnetic disturbance from the IMAGE magnetometers at 2045:30 UT.

to a regular grid, using a simple inverse distance scheme. (In detail, we used $F(\vec{r}_{int}) = \sum w_i z_i$, with $w_i = |\vec{r}_{int} - \vec{r}_i|^{-p} / (\sum |\vec{r}_{int} - \vec{r}_i|^{-p})$, $p = 3/2$, and $i=1,...,n_{obs}$, where n_{obs} is the number of observations, z_i is the observational data at the points $\vec{r}_i$, and $F(\vec{r}_{int})$ is the interpolated quantity at the interpolation point $\vec{r}_{int}$ of our grid.) This grid, defining the analysis area on which the ECM is applied, is the same as that used for our model. The resulting FACs (Figure 5a) on the first view appear to show almost no difference to the modeled ones (Figure 3e). Closer inspection reveals that the negative FAC gradients toward the northern and southern boundary of the analysis area are slightly underestimated owing to missing satellite data there. Using the second part of the sum in (5), we calculate $\vec{J}_{cf}$ (Figure 5b) from the FACs, which similarly shows only small differences to the modeled distribution (Figure 3f). To compute $\vec{J}_{df} = \vec{J}_{eq,ion}$, i.e., the first part of the sum in (5), from the simulated IMAGE data shown in Figure 4b, we use the upward continuation technique for magnetic disturbance fields from the ground to the ionosphere presented by *Amm and Viljanen* [1999]. This technique has been proven to be somewhat more accurate than field continuation methods based on spherical cap harmonics [e.g., *Haines and Torta*, 1994], which would, however, also be applicable. The resulting currents $\vec{J}_{df}$ (Figure 5c) again show very little difference to the ones following directly from the model (Figure 3g). However, small deviations exist owing to the limited amount of information provided by a finite number of magnetometers. Especially, near the boundaries of the analysis region, $\vec{J}_{df}$ is slightly overestimated. Using (1), i.e., adding the two parts of the sum in (5), we obtain a result for $\vec{J}$

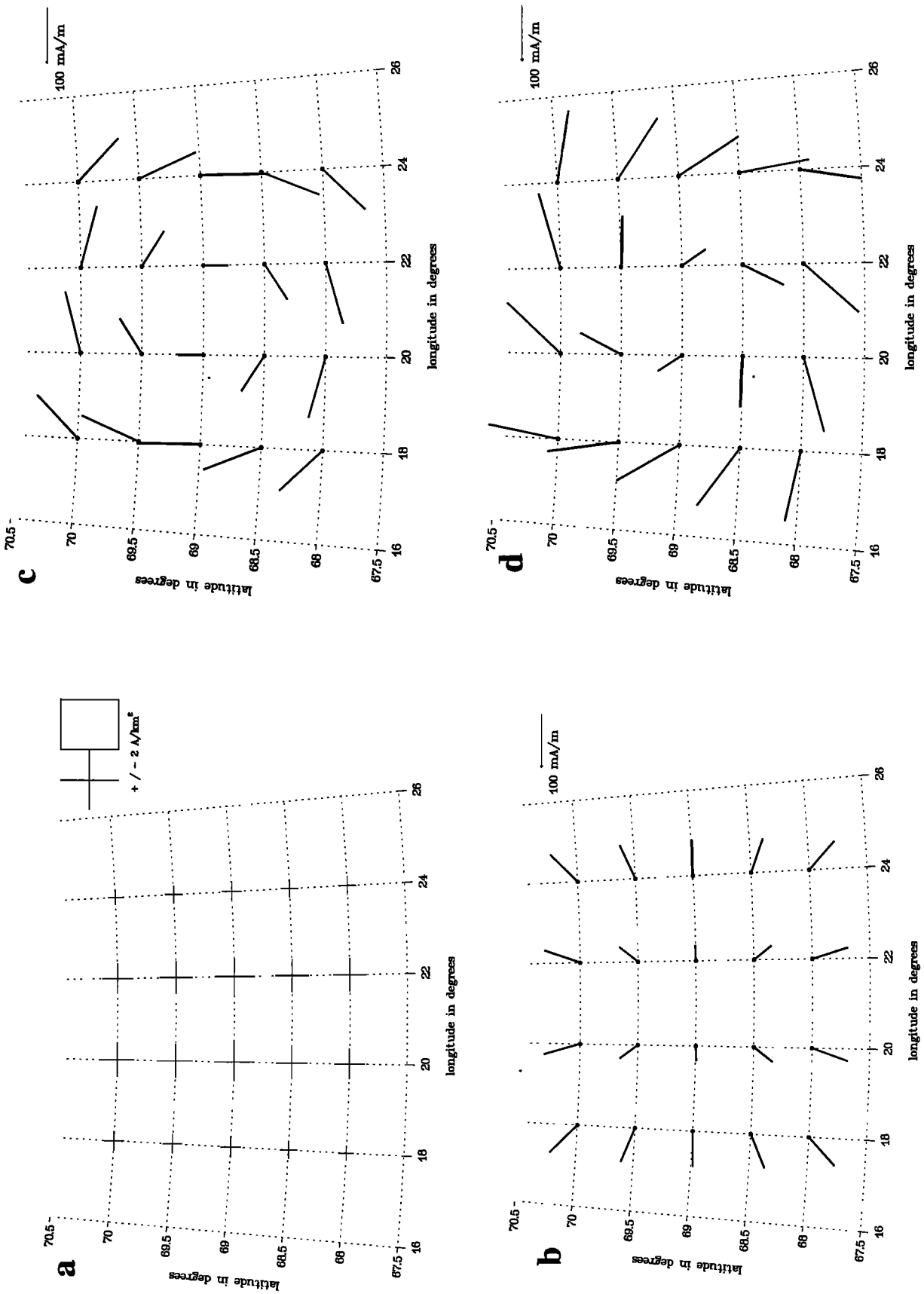

Figure 5. Results of the elementary current method. (a) Held-aligned currents $j_{\parallel}$. (b) Curl-free current part $\vec{J}_{cf}$. (c) Divergence-free current part $\vec{J}_{df}$. (d) True ionospheric currents $\vec{J}$. (e) Hall conductance Σ_H (in Siemens). (f) Pedersen conductance Σ_P (in Siemens).

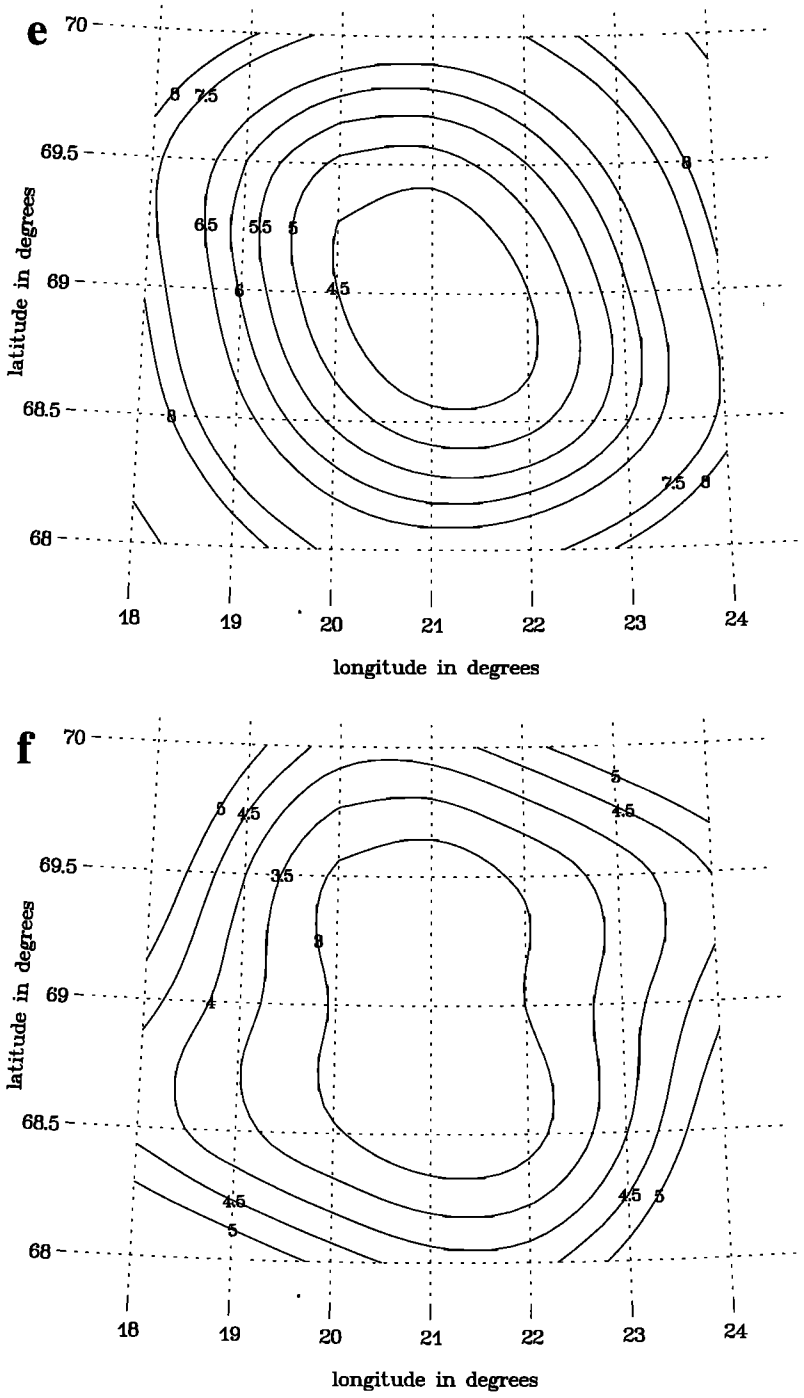

Figure 5. (continued)

from the ECM (Figure 5d), in excellent agreement with the modeled, "true" distribution (Figure 3d). Clearly, the spiralic structure of $\vec{J}$ is correctly reproduced both concerning the directions and concerning the magnitudes of the vectors.

Finally, for the case that the plasma vortex electric field (Figure 3a) was measured by the STARE coherent scatter radar (see Figure 2), we can apply (8) to calculate Σ_H and Σ_P directly from our previous results. It should be noted that because of the cross and scalar products in (8), small errors in the direction of the resulted $\vec{J}$ distribution can cause more clearly visible errors in Σ_H and Σ_P, respectively, especially in areas where $|\vec{E}|$ is small. Still, the resulting conductance distributions (Figure 5e and f) represent the Σ_H and Σ_P minima associated with the plasma vortex remarkably well, and they also reproduce the correct minimum values very closely.Because of the small deviations mentioned between the modeled and the resulted $\vec{J}_{cf}$ and $\vec{J}_{df}$, some errors are introduced near the boundaries of the analysis region, although even there the errors are less than 1.5 S. Some deviations from the isotropy with respect to the vortex's center are seen especially in the Σ_P result.

5. Summary and Conclusions

We presented the elementary current method (ECM) to obtain two-dimensional distributions of true ionospheric currents from simultaneous field-aligned current measurements by a fleet of satellites and ground-based measurements of magnetic disturbances

by an array of magnetometers. In the case that spatial observations of the ionospheric electric field are available, both the Hall and the Pedersen conductance distributions were also inferred. In contrast to most other methods that compute macroscopic ionospheric electrodynamic parameters, none of the input parameters need to be assumed.

The ECM procedure in short is the following: From satellite measurements and mapping to low altitude, the field-aligned current distribution is obtained. This is equivalent to the horizontal divergence of the ionospheric current (equation (2)). Ground magnetic records, on the other hand, can be used to compute the equivalent currents in the ionosphere. The curl of this current is equal to the curl of the ionospheric currents (equation (3)). From the knowledge of the curl and divergence of the true ionospheric currents, its spatial distribution can be constructed (equation (4)). The procedure is fairly easy to implement numerically, especially in the form for a regular grid (equation (5)), since no differential equations have to be carried out nor integrals have to be solved explicitly, but merely weighted elementary functions need to be added.

The ECM was tested using an ionospheric electrodynamic situation of a plasma vortex, modeled with respect to a real event analyzed by *Kosch et al.* [2000], and using a realistic magnetic footpoint geometry of a Cluster II passage over northern Scandinavia. Using the simulated FAC measurements by the satellites together with the IMAGE ground magnetometer observations following from our model as an input to the ECM, the method is able to reconstruct the modeled, "true" ionospheric current system with excellent accuracy, both regarding its spiralic structure, which is largely different from the structure of the equivalent currents observed by magnetometers alone, as well as regarding its magnitude. For the case that the electric field is spatially measured by the STARE radar, our results for the Pedersen and Hall conductances reproduce the modeled conductance minima in the vortex's center well, and errors remain smaller than 1.5 S in magnitude. The largest relative error amounts to 15%, but on average, relative errors are around 5%.

It should be stressed that the applicability of the ECM covers a wide range of geophysical situations and geographical locations and is not restricted to the special event or locational choices made for the test in this paper. Besides its use with Cluster II passages over the MIRACLE network for mesoscale-region analyses, excellent conjugacy opportunities with Cluster II exist for other two-dimensional ground magnetometer networks like the Canadian Auroral Network for the OPEN Program Unified Study (CANOPUS) [*Rostoker et al.*, 1994], the Magnetometer Array for Cusp and Cleft Studies (MACCS) [*Engebretson et al.*, 1995], or the Greenland magnetometers [e.g., *Stauning*, 1995]. If the geophysical situation to be analyzed is sufficiently stationary, also somewhat larger analysis regions than the one used in this paper can be used. For example, a combination of the magnetometers mentioned above could be used to infer the true currents of a large portion of the auroral ionosphere during steady convection events, when the Cluster II footpoint geometry is favorable. Another example for a geophysical target might be the midnight auroral gap for which true current distributions have been thus far difficult to obtain because of the absence of spatial electric field measurements. Although, at present, Cluster II is the only mission that can provide multipoint satellite input data as used for the ECM, the same method will be useful for possible future multisatellite missions, especially with low-altitude orbits, as well.

Spatial measurements of the ionospheric electric field used to obtain the Hall and Pedersen conductance distributions from the ECM are, in addition to the STARE radar, available from the Super Dual Auroral Radar Network (SuperDARN) radars that increasingly cover large parts of the northern and also of the southern auroral ionosphere. However, this possibility is restricted to the case that sufficient backscatter is received by the radars to reliably construct two-dimensional electric field vector results for the analysis region.

Acknowledgments The author would like to thank T.I. Pulkkinen, A. Viljanen, P. Janhunen, and K. Kauristie (all Helsinki) for their comments on the manuscript. This work was supported by a DAAD postdoctoral fellowship HSP III financed by the German Federal Ministry for Research and Technology, and by the Academy of Finland.

Michel Blanc thanks Christophe Peymirat and Takesi Iijima for their assistance in evaluating this paper.

References

Akasofu, S.-I., J. Kisabeth, B.-H. Ahn, and G.J. Romick, The S_q^p magnetic variation, equivalent current, and field-aligned current distribution obtained from the IMS Alaska meridian chain of magnetometers, *J. Geophys. Res., 85*, 2085, 1980.

Amm, O., Direct determination of the local ionospheric Hall conductance distribution from two-dimensional electric and magnetic field data: Application of the method using models of typical ionospheric electrodynamic situations, *J. Geophys. Res., 100*, 21,473, 1995.

Amm, O., Comment on "A three-dimensional, iterative mapping procedure for the implementation of an ionosphere-magnetosphere anisotropic Ohm's law boundary condition in global magnetohydrodynamic simulations" by Michael L. Goodman, *Ann. Geophys., 14*, 773, 1996.

Amm, O., Ionospheric elementary current systems in spherical coordinates and their application, *J. Geomagn. Geoelectr., 49*, 947, 1997.

Amm, O., Method of characteristics in spherical geometry applied to a Harang discontinuity situation, *Ann. Geophys., 16*, 413, 1998.

Amm, O., and A. Viljanen, Ionospheric disturbance magnetic field continuation from the ground to the ionosphere using spherical elementary current systems, *Earth Planet. Space, 51*, 431, 1999.

Baumjohann, W., R.J. Pellinen, H.J. Opgenoorth, and E. Nielsen, Joint two-dimensional observations of ground magnetic and ionospheric electric fields associated with local auroral break-ups, *Planet. Space Sci., 29*, 431, 1981.

Engebretson, M.J., W.J. Hughes, J.L. Alford, E. Zesta, L.J. Cahill Jr., R.L. Arnoldy, and G.D. Reeves, Magnetometer array for cusp and cleft studies observations of the spatial extent of broadband ULF magnetic pulsations at cusp/ cleft latitudes, *J. Geophys. Res., 100*, 19,741, 1995.

Haines, G.V., and J.M. Torta, Determination of equivalent current sources from spherical cap harmonic models of geomagnetic field variations, *Geophys. J. Int., 118*, 499, 1994.

Iijima, T., and T.A. Potemra, Large-scale characteristics of field-aligned currents at northern high latitudes observed by Triad, *J. Geophys. Res., 83*, 2165, 1978.

Inhester, B., J. Untiedt, M. Segatz, and M. Kürschner, Direct determination of the local ionospheric Hall conductance distribution from two-dimensional electric and magnetic field data, *J. Geophys. Res., 97*, 4073, 1992.

Kamide, Y., A.D. Richmond, and S. Matsushita, Estimation of ionospheric electric fields, ionospheric currents and field-aligned currents from ground magnetic records, *J. Geophys. Res., 86*, 801, 1981.

Kamide, Y., et al., Global distribution of ionospheric and field-aligned currents during substorms as determined from six IMS meridian chains of magnetometers: Initial results, *J. Geophys. Res., 87*, 8228, 1982.

Kosch, M.J., O. Amm, and M.W.J. Scourfield, A plasma vortex revisited: The importance of including ionospheric conductivity measurements, *J. Geophys. Res., 105*, 24,889, 2000.

Lester, M., J.A. Davies, and T.S. Virdi, High-latitude Hall and Pedersen conductances during substorm activity in the SUNDIAL-ATLAS campaign, *J. Geophys. Res., 101*, 26,719, 1996.

Murison, M., A.D. Richmond, and S. Matsushita, Estimation of ionospheric electric fields and currents from a regional magnetometer array, *J. Geophys. Res., 90*, 3525, 1985.

Opgenoorth, H.J., R.J. Pellinen, W. Baumjohann, E. Nielsen, G. Marklund, and L. Eliasson, Three-dimensional current flow and particle precipitation in a westward traveling surge (observed during the Barium-GEOS rocket experiment), *J. Geophys. Res., 88*, 3138, 1983.

Rich, F.J., and Y. Kamide, Convection electric fields and ionospheric

currents derived from model field-aligned currents at high latitudes, *J. Geophys. Res., 88*, 271, 1983.

Richmond, A.D., and Y. Kamide, Mapping electrodynamic features of the high-latitude ionosphere from localized observations: Technique, *J. Geophys. Res., 93*, 5741, 1988.

Rostoker, G., J.C. Samson, F. Creutzberg, T.J. Hughes, D.R. McDiarmid, A.G. McNamara, A. Vallance Jones, D.D. Wallis, and L.L. Cogger, CANOPUS: A ground based array for remote sensing the high latitude ionosphere during the ISTP/GGS program, *Space Sci. Rev., 71*, 743, 1994.

Stauning, P., Progresing IMF B_Y-related polar ionospheric convection disturbances, *J. Geomagn. Geoelectr., 47*, 735, 1995.

Sulzbacher, H., W. Baumjohann, T.A. Potemra, E. Nielsen, and G. Gustafsson, Observations of ionospheric and field-aligned currents in the late afternoon sector with Triad and the Scandinavian Magnetometer Array, *J. Geophys., 51*, 55, 1982.

Syrjäsuo, M., et al., Observations of substorm electrodynamics using the MIRACLE network, in *Substorms-4*, edited by S. Kokubun and Y. Kamide, Terra Scientific Publishing Company, Tokyo, p. 111-114, 1998.

Untiedt, J., and W. Baumjohann, Studies of polar current systems using the IMS Scandinavian magnetometer array, *Space Sci. Rev., 63*, 245, 1993.

O. Amm, Finnish Meteorological Institute, Geophysical Research Division, P.O. Box 503, FIN-00101 Helsinki, Finland. (Olaf.Amm@fmi.fi)

(Received October 20, 2000; revised January 8, 2001;
accepted January 26,2001.)